



1 An improved process-oriented hydro-biogeochemical model for 2 simulating dynamic fluxes of methane and nitrous oxide in alpine 3 ecosystems with seasonally frozen soils

4 Wei Zhang¹, Zhisheng Yao¹, Siqi Li¹, Xunhua Zheng^{1, 2}, Han Zhang^{1, 3}, Lei Ma^{1, 4}, Kai Wang¹, Rui
5 Wang¹, Chunyan Liu¹, Shenghui Han¹, Jia Deng⁵, Yong Li⁶

6 ¹State Key Laboratory of Atmospheric Boundary Layer Physics and Atmospheric Chemistry, Institute of Atmospheric
7 Physics, Chinese Academy of Sciences, Beijing 100029, P. R. China

8 ²College of Earth and Planetary Science, University of Chinese Academy of Sciences, Beijing 100049, P. R. China

9 ³School of Geographic and Environmental Sciences, Tianjin Normal University, Tianjin 300387, P. R. China

10 ⁴Institute of Meteorology and Climate Research, Atmospheric Environmental Research (IMK-IFU), Karlsruhe Institute of
11 Technology, Kreuzackbahnstrasse 19, 82467 Garmisch-Partenkirchen, Germany

12 ⁵Complex Systems Research Center, Institute for the Study of Earth, Oceans and Space, University of New Hampshire, 39
13 College Road, Durham, NH 03824, USA

14 ⁶Key Laboratory of Agro-ecological Processes in Subtropical Region, Institute of Subtropical Agriculture, Chinese Academy
15 of Sciences, Hunan 410125, P. R. China

16

17 *Correspondence to:* Xunhua Zheng (xunhua.zheng@post.iap.ac.cn)

18 **Abstract.** To evaluate the sustainability of terrestrial ecosystems, the hydro-biogeochemical model Catchment Nutrient
19 Management Model - DeNitrification-DeComposition (CNMM-DNDC) was established to simultaneously quantify
20 ecosystem productivity and losses of nitrogen and carbon at the site or catchment scale. As a process-oriented model, this
21 model is expected to be universally applied to different climate zones, soils, land uses and field management practices. This
22 study, as one of many efforts to fulfil such an expectation, was performed to improve the CNMM-DNDC by incorporating a
23 physical-based soil thermal module to simulate the soil thermal regime in the presence of freeze-thaw cycles. The modified
24 model was validated with simultaneous field observations in three typical alpine ecosystems (wetlands, meadows and forests)
25 within a catchment located in the seasonally frozen region of the eastern Tibetan Plateau. Then, the model was further
26 applied to evaluate its performance in simulating the effects of alpine wetland degradation on methane (CH₄) and nitrous
27 oxide (N₂O) fluxes. The validation showed that the modified CNMM-DNDC was able to simulate the observed seasonal
28 dynamics of soil temperature, moisture, and fluxes of CH₄ and N₂O in the three typical alpine ecosystems, with index of
29 agreement values of 0.91–1.00, 0.49–0.83, 0.57–0.88 and 0.26–0.47, respectively. Consistent with the emissions determined
30 from the field observations, the simulated aggregate emissions of CH₄ and N₂O were significantly reduced due to wetland
31 degradation and were dominated by a reduction in CH₄ emissions. This study indicates the potential for utilizing the process-
32 oriented model CNMM-DNDC to predict hydro-biogeochemical processes, as well as related gas emissions, in seasonally
33 frozen regions. As the original CNMM-DNDC was previously validated in some unfrozen regions, the modified CNMM-



34 DNDC could be applied to evaluate the sustainability of various ecosystems under different climates, soils and field
35 management practices at the site or catchment scale.

36 **1 Introduction**

37 The elements of nitrogen and carbon are essential components of ecosystems (e.g., Breuer *et al.*, 2010; Canfield *et al.*,
38 2010). Climate changes due to warming and human anthropogenic activities derived from food production have significantly
39 altered the cycling of nitrogen and carbon and led to increased reactive nitrogen availability and carbon losses, which result
40 in a series of environmental problems at the catchment, regional and even global scales (e.g., Galloway *et al.*, 2004;
41 Galloway *et al.*, 2008; Ju *et al.*, 2009). Excessive reactive nitrogen in soils can be lost in the forms of nitrogen gases, such as
42 nitrous oxide (N₂O), nitric oxide (NO) and ammonia (NH₃), and nitrogen pollution, such as nitrate (NO₃⁻) and ammonium
43 (NH₄⁺), in water through leaching or surface runoff (e.g., Seitzinger, 2008; Collins *et al.*, 2016). In the face of increased air
44 temperatures and intensive land use changes, especially in cold regions, the soil organic carbon stored during long periods
45 has been lost to the atmosphere via methane (CH₄) and carbon dioxide (CO₂) (e.g., Piao *et al.*, 2009; Fenner and Freeman,
46 2011; Schuur *et al.*, 2015). These nitrogen and carbon losses contribute to potential global warming (CO₂, CH₄ and N₂O), air
47 pollution (NO and NH₃) and surface/groundwater pollution (NO₃⁻ and NH₄⁺). Therefore, sustainable ecosystems urgently
48 need to be established that not only focus on net primary productivity but also are friendly to the environment with the
49 minimal hazards, including greenhouse gases, air pollution and water pollutants (e.g., Cui *et al.*, 2018; Zhang *et al.*, 2019).

50 The cycling of nitrogen and carbon is closely related to soil water processes (e.g., Breuer *et al.*, 2010; Vereecken *et al.*,
51 2016; Zhang *et al.*, 2018). Thus, interactions among soil waters and the cycling of nitrogen and carbon govern biological
52 productivity and environmental outcomes (e.g., Zhu *et al.*, 2018). The interactions consist of the redox potential for different
53 transformation processes influenced by the spatiotemporal variation in soil water content and the lateral transport of water
54 and dissolved nitrogen or carbon controlled by surface and subsurface flow (e.g., McClain *et al.*, 2003; Castellano *et al.*,
55 2013; Bechmann, 2014). For example, the variation in soil water content can create hot spots or moments of nitrogen and
56 carbon losses by influencing plant nitrogen uptake, redox potential, and the transport of dissolved nitrogen and carbon (e.g.,
57 Zhu *et al.*, 2012; Keiluweit *et al.*, 2017). Therefore, a complete understanding of biogeochemical processes will inevitably
58 involve interactions among soil water and the cycling of nitrogen and carbon (e.g., Breuer *et al.*, 2010; Vereecken *et al.*,
59 2016; Zhu *et al.*, 2018).

60 Biogeochemical models, such DNDC, WNMM, CENTURY and DayCent, are effective tools for simulating the
61 cycling of nitrogen and carbon and quantifying the effects of climate change and human anthropogenic activities on
62 ecosystems (e.g., Foereid *et al.*, 2007; Li, 2007; Li *et al.*, 2007; Cheng *et al.*, 2014). However, comprehensive hydrological
63 processes, especially for the lateral transport of water and nutrients, are generally simplified or ignored in these models due
64 to specific questions that must be addressed (e.g., Li, 2007; Li *et al.*, 2007; Chen *et al.*, 2008; Deng *et al.*, 2014). On the
65 other hand, land surface or hydrological models at large scales, which are designed with explicit mechanisms of hydrology,



66 generally focus on vertical and lateral nutrient transport, such as nitrate loads into rivers (e.g., Liu *et al.*, 2019). However, the
67 simulations of nitrogen and carbon processes are usually based on empirical functions even without predicting gas loss. Due
68 to the various purposes of different models, coupling soil hydrological models with biogeochemical models can be an
69 effective strategy for integrating soil water and cycling of nitrogen and carbon to improve model performance. Thus, the
70 coupled model with improved performance can be applied to evaluate the sustainability of natural or agricultural ecosystems,
71 simultaneously predicting productivity and potential negative environmental effects (e.g., Zhang *et al.*, 2018; Zhu *et al.*,
72 2018).

73 In recent years, efforts have been implemented to couple models, such as SWAT-N, LandscapeDNDC-CMF, APSIM,
74 SWAT-DayCent, and CNMM-DNDC (e.g., Pohlert *et al.*, 2007; Haas *et al.*, 2012; Holzworth *et al.*, 2014; Wu *et al.*, 2016;
75 Zhang *et al.*, 2016; Zhang *et al.*, 2018). The models derived from SWAT were all based on semi-distributed hydrological
76 models using hydrologic response units and did not perform better in estimating non-point source pollution (e.g., Pohlert *et al.*,
77 2007; Bosch *et al.*, 2011; Wu *et al.*, 2016). A coupler was used to couple two models for LandscapeDNDC-CMF (e.g.,
78 Haas *et al.*, 2012; Schroeck *et al.*, 2019). Compared with other models, the Catchment Nutrient Management Model -
79 DeNitrification-DeComposition (CNMM-DNDC), which was established by incorporating the core biogeochemical
80 processes of DNDC into the hydrological framework of the CNMM, was validated at a catchment with complex landscapes
81 in the subtropical region and showed good performance for simultaneously simulating various variables, including
82 ecosystem productivity, hydrological nitrogen losses and nitrate discharge in streams, and emissions of gaseous carbon and
83 nitrogenous gases (Zhang *et al.*, 2018). Therefore, the CNMM-DNDC has the capacity to evaluate the sustainability of
84 ecosystems with simultaneous simulations of various variables closely related to both productivity and environmental
85 hazards.

86 However, as a process-oriented hydro-biogeochemical model designed to be applicable to different climate zones, soils,
87 land uses and field management practices, CNMM-DNDC testing is still lacking due to limited observations for model
88 validation. In this study, the model was applied to a catchment in seasonally frozen regions located on the eastern Tibetan
89 Plateau (TP) with the land use types of alpine wetlands, meadows and forests to test its ability to simulate hydro-
90 biogeochemical processes. However, scientific descriptions of soil thermal dynamics due to freeze-thaw cycles are still
91 lacking for the CNMM-DNDC. This gap may hinder model application in seasonally frozen regions, which account for 56%
92 of the exposed land surface of the Northern Hemisphere (Jiang *et al.*, 2020). In addition, the soil freeze-thaw cycles that
93 occur in these mid-high latitude regions exert important influences on soil thermal dynamics, as well as on related
94 hydrological processes, thus increasing the availability of substrates and stimulating the processes of CH₄ and N₂O
95 production and emissions in soils (e.g., Song *et al.*, 2019). Therefore, we hypothesize that adding the missing scientific
96 processes of soil thermal dynamics into the internal model program codes can improve the performance of the CNMM-
97 DNDC in simulating the soil thermal dynamics, hydrological processes and CH₄ and N₂O fluxes in seasonally frozen regions.
98 Filling this gap is especially necessary to broaden model applicability.



99 To test the above hypothesis, the catchment simulation in the Rierlangshan was conducted using a unique experimental
100 dataset, which was obtained by Zhang *et al.* (2018a, 2019) and Yao *et al.* (2019) for the catchment that involved three typical
101 alpine ecosystems, wetlands, meadows and forests, on the eastern TP. The aims of this study were to (i) attempt to address
102 the gap in the CNMM-DNDC by improving the scientific processes of soil thermal dynamics for seasonally frozen regions;
103 (ii) compare the performances of the original and modified models in simulating the soil profile temperature, topsoil
104 moisture and CH₄ and N₂O fluxes in three typical alpine ecosystems in the Rierlangshan catchment with field observations,
105 and (iii) evaluate the model performance in simulating the effects of wetland degradation on CH₄ and N₂O fluxes. Therefore,
106 the validated model with modifications provides a mechanism for not only interpreting observations but also predicting the
107 CH₄ and N₂O fluxes in alpine ecosystems.

108 2 Materials and methods

109 2.1 Model description

110 2.1.1 Overview of the CNMM-DNDC model

111 The CNMM-DNDC is a process-oriented model developed for simulating hydro-biogeochemical interactions at the
112 catchment or site scale, and this model is designed following the basic theories of physics, chemistry, and biogeochemistry
113 and has the capacity to simulate the complex transport and transformation of water, nitrogen and carbon in terrestrial
114 ecosystems under both aerobic and anaerobic conditions. The model can be applied to simultaneously quantify ecosystem
115 productivity, net emissions of nitrogen and carbon gases and hydrological nitrogen losses through soil leaching and
116 discharge in streams from an entire catchment or individual landscape unit (Zhang *et al.*, 2018b).

117 The model was established to address the bottleneck issue associated with most biogeochemical models, i.e., the
118 inability to simulate the lateral flows of water and nutrients, by incorporating the core biogeochemical processes of DNDC
119 (including the processes of decomposition, nitrification, denitrification and fermentation) into the hydrological framework of
120 the CNMM. In the CNMM-DNDC, the processes related to the production of N₂O include nitrification and denitrification,
121 which occur simultaneously at aerobic and anaerobic microsites, respectively. The concept of an “anaerobic balloon” was
122 adopted to determine the microsites and allocate substrates for nitrification and denitrification. The sizes of the aerobic
123 (nitrification) and anaerobic (denitrification) microsites were determined by the soil redox potential (Eh) using the Nernst
124 equation (Li, 2007). The “hole in the pipe” concept was applied to calculate N₂O production during nitrification, which is
125 influenced by the soil moisture, temperature and pH. The production of N₂O during denitrification was predicted with
126 Michaelis-Menten kinetics and Pirt functions following the reaction chain of denitrification. The predicted CH₄ flux was
127 influenced by CH₄ production, oxidation and transportation. Methane production and oxidation occurred simultaneously and
128 were determined by the sizes of yhr aerobic (production) and anaerobic (oxidation) microsites, which were defined by an Eh
129 calculator in terms of an “anaerobic balloon” (“CH₄ balloon”). The predicted CH₄ production was calculated from the carbon



130 substrates resulting from decomposed soil organic carbon (SOC) and plant root biomass with the effects of soil temperature.
 131 Three pathways of CH₄ transportation in soils were included in the model: plant-mediated transport, ebullition and diffusion.
 132 For more details, please see Li. (2007) and Zhang *et al.* (2018b).

133 2.1.2 Modifications of the CNMM-DNDC model

134 In this study, to replace the original thermal module that involved simple parameterizations with a physically based
 135 model describing the soil thermal regime in the presence of freeze-thaw cycles, the Northern Ecosystem Soil Temperature
 136 model was incorporated into the CNMM-DNDC at the code level (Zhang *et al.*, 2003). The modified model explicitly
 137 described the energy exchange within the soil-vegetation-atmosphere system and the active layer dynamics (Zhang *et al.*,
 138 2003; Deng *et al.*, 2014). These modifications are indispensable for accurately simulating freeze-thaw cycles in seasonally
 139 frozen regions, which are crucial for characterizing the active layer and soil thermal dynamics, soil hydrology and nitrogen
 140 or carbon cycling in these regions.

141 The thermal dynamics of the soil and snow were calculated by the one-dimensional heat conduction equation (Eq. 1),
 142 which was solved numerically using Eqs. 2–4. In the above equations, C (J m⁻³ °C⁻¹), k (W m⁻¹ °C⁻¹), T (°C) and G (W m⁻²)
 143 denote the soil heat capacity, thermal conductivity, soil temperature and heat fluxes between layers, respectively. Both Z and
 144 D are the thicknesses of the soil layer (m), Δt is the time step of the calculation, and l denotes the soil layer l . S is the internal
 145 heat exchange due to freezing or thawing (W m⁻³) when the soil temperature is around 0 °C. The soil temperature changes
 146 affected by freezing or thawing were determined on the basis of energy conservation, which indicated that the latent heat
 147 released during freezing equalled the amount of heat required for the increased soil temperature and vice versa. The soil heat
 148 capacity (C , J m⁻³ °C⁻¹) is the weighted average of five constituents in the volumetric fraction (θ), including organic matter
 149 (2.5×10^6), minerals (2.0×10^6), water (4.2×10^6), ice (2.1×10^6) and air (1.2×10^3) (Eq. 5). The thermal conductivity (k , W m⁻¹
 150 °C⁻¹) is the geometric mean of the thermal conductivities of the above five constituents (Eq. 6), with values of 0.25, 2.9,
 151 0.57, 2.2 and 0.025 W m⁻¹ °C⁻¹ for organic matter, minerals, water, ice and air, respectively. The upper and lower boundary
 152 conditions of the thermal dynamics were determined by the surface energy balance and the defined geothermal heat flux at a
 153 soil depth of 35 m.

$$C \frac{\partial T}{\partial t} = \frac{\partial}{\partial Z} \left(k \frac{\partial T}{\partial Z} \right) + S \quad (1)$$

$$C_l \frac{\Delta T_l}{\Delta t} = \frac{G_{l-1,l} - G_{l,l+1}}{D_l} + S_l \quad (2)$$

$$G_{l-1,l} = \frac{(0.5k_l + 0.5k_{l-1})(T_{l-1} - T_l)}{0.5D_{l-1} + 0.5D_l} \quad (3)$$

$$G_{l,l+1} = \frac{(0.5k_l + 0.5k_{l+1})(T_l - T_{l+1})}{0.5D_l + 0.5D_{l+1}} \quad (4)$$

$$C_l = \sum_{j=1}^5 C_{l,j} \theta_{l,j} \quad (5)$$

$$k_l = \prod_{j=1}^5 k_{l,j}^{\theta_{l,j}} \quad (6)$$



154 Descriptions of the processes related to soil thermal dynamics are detailed in Zhang *et al.* (2018b). The modified
155 CNMM-DNDC was able to simulate the thermal dynamics in seasonally frozen regions as well as their impacts on
156 biogeochemical processes, especially the emissions of nitrogen and carbon gases.

157 2.2 Catchment and field descriptions

158 The study area is the Rierlangshan catchment (34°02'N, 102°43'E) on the eastern TP with an area of 189 ha (Yao *et al.*,
159 2019). This catchment is located in the source region of the Pai-Lung River, which is a sub-branch of the upper Yangtze
160 River (Zhang *et al.*, 2018a). This region is subject to a cold humid continental monsoon climate, and it had an annual mean
161 air temperature of 1.6 ± 0.7 °C and average annual precipitation of 649 ± 94 mm in 1980–2012 as observed at the Zoige
162 Meteorological Station (~80 km south of the catchment) (Ma *et al.*, 2018). The catchment consists of alpine wetlands,
163 meadows and forests (Yao *et al.*, 2019). The alpine wetlands in the catchment are part of the Zoige wetland and are degraded
164 due to anthropogenic drainage and climate warming (Dong *et al.*, 2010; Li *et al.*, 2014). Degraded alpine wetlands are
165 commonly distributed throughout the Zoige wetland, and nearly 83% of the permanently inundated wetlands have been
166 converted into “wet grassland” (Xiang *et al.*, 2009; Li *et al.*, 2014).

167 CH₄ and N₂O fluxes were manually measured weekly or twice per week using the gas chromatograph-based static
168 opaque chamber method at three sites in alpine wetlands (34°02'6.53"N, 102°43'29.66"E, 3304 m a.s.l.), meadows
169 (34°02'01"N, 102°43'28"E, 3326 m a.s.l.) and forests (34°01'47.13"N, 102°44'0.87"E, 3415 m a.s.l.) in the Rierlangshan
170 catchment from 2013 to 2015 (Zhang *et al.*, 2018a; Yao *et al.*, 2019; Zhang *et al.*, 2019) (Fig. S1). The alpine meadow site is
171 located on a north-facing slope with a slope gradient of 11 ° and neighbours the alpine wetland site at the slope base with a
172 gentle slope of 2 °. In addition, soil temperatures at different depths and topsoil moisture in the alpine wetlands, meadows and
173 forests were observed daily and twice per week, respectively. The details regarding the field observations of the CH₄ and
174 N₂O fluxes and the relevant auxiliary variables are described in Zhang *et al.* (2018a), Yao *et al.* (2019), Zhang *et al.* (2019)
175 and Table S1 (online supplementary materials).

176 2.3 Model simulation

177 The modified CNMM-DNDC was applied in the Rierlangshan catchment with the three alpine ecosystems: wetlands,
178 meadows and forests. The dataset required for the catchment simulation included (1) a digital elevation model (DEM) with a
179 resolution of 30×30 m² from the geospatial data cloud (Fig. S1; <http://www.gscloud.cn/>); (2) a map of alpine ecosystems,
180 including wetlands, meadows and forests; (3) a climate dataset of hourly weather data (air temperature, precipitation, wind
181 speed, solar radiation, longwave radiation, and humidity), which were obtained from the meteorological station in the target
182 catchment for the years with field observations (2013.11–2015.10) and were adapted from the daily data at the Zoige
183 Meteorological Station (provided by the National Meteorological Information Center: <http://data.cma.cn/>; last access: 10th
184 June, 2020) for other years; (4) a soil properties dataset of the observed clay fraction, organic matter content, total nitrogen,
185 pH and bulk density of the three alpine ecosystems in 1 m soil profile (Ma *et al.*, 2018; Zhang *et al.*, 2018a; Yao *et al.*, 2019;



186 Zhang *et al.*, 2019); and (5) a management practices dataset including grazing time and intensity for the alpine wetlands and
187 meadows. In addition, other required soil inputs of field capacity, wilting point and saturated hydrological conductivity were
188 calculated by pedo-transfer functions (Li *et al.*, 2019). The simulated soil profile (0–35 m depth) was divided into 23 layers.
189 The thicknesses of the top 20 layers were 1, 5 and 10 cm for the top 10 layers, middle 2 layers, and other 8 layers,
190 respectively. The thicknesses of the last three layers were 0.5, 3.5 and 31 m. The geothermal heat flux in the catchment was
191 estimated at 0.053 W m^{-2} (Pollack and Chapman, 1977). Therefore, using the database, a catchment simulation of hydro-
192 biogeochemical processes was performed with spatial and temporal resolutions of $30 \times 30 \text{ m}^2$ and 3 hours, respectively, by the
193 modified CNMM-DNDC.

194 2.4 Statistics and analysis

195 The statistical criteria applied for evaluating the model performance in this study included (i) the index of agreement
196 (IA), (ii) the Nash–Sutcliffe index (NSI), (iii) the determination coefficient (R^2) and slope of the zero-intercept univariate
197 linear regression (ZIR) of the observations against the simulations, and (iv) the model relative bias (MRB) (e.g., Nash and
198 Sutcliffe, 1970; Willmott and Matsuura, 2005; Moriasi *et al.*, 2007; Congreves *et al.*, 2016; Jiang, 2010; Dubache *et al.*,
199 2019). A value of IA (0–1) closer to 1 showed a better simulation ranging from 0 to 1. An NSI value (ranging from minus
200 infinity to 1) closer to 1 was better. Better model performance was indicated by a slope and an R^2 value that were both closer
201 to 1 in a significant ZIR. For more details on these criteria, refer to the online supplementary materials (Eqs. S1–4 in Table
202 S2). In addition, the SPSS Statistics Client 19.0 (SPSS Inc., Chicago, USA) and Origin 8.0 (OriginLab, Northampton, MA,
203 USA) software packages were applied for the statistical analysis and graphical comparison.

204 3 Results

205 3.1 Model validation

206 3.1.1 Soil temperature and moisture

207 The simulated soil profile temperatures of the three typical alpine ecosystems were significantly improved by
208 including the scientific processes of soil thermal dynamics suitable for seasonally frozen regions (Figs. 1 and S2). The
209 simulated seasonal dynamics and magnitudes were consistent with those from the field observations for various soil depths,
210 with IA, NSI, and ZIR slopes and R^2 values of 0.91–1.00, 0.68–0.99, 0.83–1.09 and 0.73–1.00 for the three alpine
211 ecosystems, respectively (Table 1). For the observed alpine wetlands and meadows, the simulation showed that the freezing
212 of soil started in early November and continued to the end of April in the next year. The frozen depth reached a maximum in
213 the middle of February. However, the simulated maximum frozen depths for the observed alpine meadows (0.69–0.74 m)
214 were approximately double those for the alpine wetlands (0.30–0.39 m) (Fig. S3).



215 For the topsoil moisture, the simulated soil moisture dynamics were comparable to those from the field observations,
216 with IA and NSI values of 0.59–0.83 and -0.94–0.32 for the three alpine ecosystems, respectively (Fig. 2 and Table 1). In
217 comparison to the other alpine ecosystems, the alpine wetlands had higher soil moisture, which ranged from 0.41 to 0.98 and
218 from 0.38 to 0.93 for the observations and simulations in the water-filled pore space (WFPS), respectively. The soil moisture
219 values of the alpine meadows and forests were highly variable and depended on the variation trend in precipitation for both
220 observations and simulations. However, an underestimation of soil moisture in the winter period occurred for both alpine
221 meadows and forests due to a possible overestimation of evapotranspiration. The performances of the modified model in
222 simulating the soil profile temperature and topsoil moisture indicate that the modified CNMM-DNDC can reliably predict
223 the soil thermal dynamics and water movement in the three alpine ecosystems at the catchment scale, which is crucial for
224 correctly simulating soil hydrology, plant growth and biogeochemical processes.

225 3.1.2 Methane fluxes

226 The daily observed CH₄ emissions from the alpine wetlands were highly variable and showed a clear seasonal cycle,
227 with intensive CH₄ emissions from May to November and weak emissions in other periods (Fig. 3a). The observed alpine
228 meadows and forests functioned exclusively as sinks of atmospheric CH₄ with higher rates of uptake during the growing
229 season and lower uptake rates in the dormant season (Figs. 4a and 5a). The original model significantly overestimated CH₄
230 emissions from the alpine wetlands. The modified CNMM-DNDC accurately identified the functions of the sources or sinks
231 in the three alpine ecosystems and generally captured the magnitude and seasonal characteristics of the daily CH₄ fluxes,
232 with an IA of 0.57–0.88 for the three alpine ecosystems (Figs. 3–5 and Table 1). However, the CH₄ uptake rates during the
233 dormant season were obviously underestimated by the modified model at both sites, especially at the alpine forest site, which
234 was responsible for the underestimation of cumulative CH₄ uptake. The observed cumulative CH₄ emissions ranged from -
235 2.60 to 33.5 kg C ha⁻¹ yr⁻¹ and the modelled values ranged from -1.90 to 31.0 kg C ha⁻¹ yr⁻¹ (Fig. 6a). These results indicate
236 that the modified CNMM-DNDC successfully simulated the CH₄ fluxes of the three typical alpine ecosystems at the
237 catchment scale and showed the capacity to predict the effects of wetland degradation on CH₄ emissions.

238 3.1.3 Nitrous oxide fluxes

239 The daily observed N₂O emissions from the alpine wetlands were higher than those from the alpine meadows but
240 lower than those from the alpine forests (Figs. 3b, 4b and 5b). Similar seasonal patterns of N₂O fluxes were observed for the
241 three alpine ecosystems with intensive emissions in the growing season. The N₂O emission peak during the dormant season
242 was observed in the alpine meadows and, was the major contributor to annual emissions. The modified CNMM-DNDC
243 generally captured the seasonal dynamics of daily N₂O fluxes with an IA of 0.26–0.47 for the three alpine ecosystems (Figs.
244 3–5 and Table 1), but the N₂O emissions from the alpine wetlands were significantly overestimated by the original model.
245 For the modified model, the simulated N₂O emissions from the alpine wetlands and forests showed obvious seasonal patterns
246 with higher emissions during the growing season, but no abrupt emission peak was captured at the end of the growing season



247 for the alpine wetlands. In addition, compared with the original model, the modified model captured the peak emissions that
248 occurred during the freeze-thaw period from the alpine meadows due to the death of microbes, but the dynamics of the peak
249 emissions were not well simulated. The observed cumulative N₂O emissions ranged from 0.14 to 0.58 kg N ha⁻¹ yr⁻¹ and the
250 modelled values ranged from 0.12 to 0.32 kg N ha⁻¹ yr⁻¹ (Fig. 6b). These results indicate that the modified CNMM-DNDC
251 showed the potential to estimate N₂O emissions in seasonally frozen regions and thus was able to assess the influences of
252 wetland degradation on N₂O emissions.

253 3.2 Annual aggregate emissions of CH₄ and N₂O

254 Annual aggregate emissions of CH₄ and N₂O in carbon dioxide (CO₂) equivalents were calculated for the three alpine
255 ecosystems from November 2013 to November 2014 for alpine wetlands and meadow and from April 2014 to April 2015 for
256 alpine forests, and the global warming potentials were 34 for CH₄ and 298 for N₂O on a 100-year time horizon (IPCC, 2013).
257 The simulated aggregate emissions by the modified model were 1.5, 0.015, and 0.061 Mg CO₂eq ha⁻¹ yr⁻¹ for the observed
258 alpine wetlands, meadows and forests, respectively, which were consistent with those from the field observations (1.6, 0.014,
259 and 0.15 Mg CO₂eq ha⁻¹ yr⁻¹ for the alpine wetlands, meadows and forests, respectively) (Fig. 6c). However, the original
260 model significantly overestimated the aggregate emissions due to the high predicted CH₄ and N₂O emissions. In comparison,
261 the degraded wetlands functioned as the sources of aggregate emissions of CH₄ and N₂O, but the aggregate emissions from
262 adjacent wet alpine meadows were much lower. Zhang *et al.* (2019) found that annual CH₄ emissions from permanently
263 inundated wetlands were 7.1 times higher than those from degraded wetlands with seasonal inundation. Assuming N₂O
264 emissions were zero for permanently inundated wetlands (e.g., Kolb and Horn, 2012; Hatano, 2019), the aggregate emissions
265 of CH₄ and N₂O were estimated at 10.8 Mg CO₂eq ha⁻¹ yr⁻¹ for natural alpine wetlands based on observations. For the
266 virtual experiment of annually inundated wetlands, the simulated aggregate emissions of CH₄ and N₂O were 7.2 Mg CO₂eq
267 ha⁻¹ yr⁻¹ with CH₄ and N₂O emissions of 158 kg C ha⁻¹ yr⁻¹ and 0.0 kg N ha⁻¹ yr⁻¹, respectively (Fig. 6). These consistent
268 results also illustrate that the modified model performed well in capturing the characteristics of the CH₄ and N₂O emissions
269 from the three typical alpine ecosystems in seasonally frozen regions. In addition, wetland degradation resulted in decreased
270 CH₄ emissions but increased N₂O emissions. However, the increased N₂O emissions could be totally offset by the reduced
271 CH₄ emissions, thus finally leading to the decreased aggregate emissions of CH₄ and N₂O from degraded wetlands than
272 permanently inundated wetlands but still much higher than those of adjacent wet alpine meadows.

273 4 Discussions

274 4.1 Model performance in simulating thermal dynamics

275 The soil freeze-thaw cycles in seasonally frozen regions determine the soil profile temperature and hydrological
276 processes, which are key factors that regulate the cycling of nitrogen and carbon (e.g., Zhang *et al.*, 2015; Hugelius *et al.*,
277 2020). Therefore, improving the scientific processes of soil thermal dynamics in the presence of active layer dynamics is



278 essential for applying the CNMM-DNDC to simulate the biogeochemical processes in seasonally frozen regions, which are
279 sensitive and vulnerable to climate change and human activities (Hatano, 2019; Hugelius *et al.*, 2020; Jiang *et al.*, 2020). The
280 original model adopted a relatively simple module with an empirical function to calculate thermal transportation within the
281 soil-vegetation-atmosphere system and did not consider the effects of freeze-thaw cycles on soil temperature and moisture.
282 The newly incorporated module was based on explicit energy conservation and exchange in the soil profile and successfully
283 captured the variations in soil temperature and topsoil moisture for the three alpine ecosystems during the freeze-thaw period.
284 Compared with other models applied in seasonally frozen regions at different scales, the modified CNMM-DNDC simulated
285 soil profile temperature influenced by soil hydrological processes equally well (e.g., Zhang *et al.*, 2002; Deng *et al.*, 2014;
286 Guo *et al.*, 2015; Jiang *et al.*, 2020). In addition, the simulated lower soil frozen depth for the observed alpine wetland was
287 primarily attributed to the higher soil profile moisture level, as the thermal conductivity and heat capacity for water-filled
288 pores were higher than those for air-filled pores. These results indicate the efficiency of the incorporated module in
289 simulating soil thermal dynamics and related hydrological processes in seasonally frozen regions.

290 **4.2 Model performance in simulating CH₄ fluxes**

291 Compared with the annually inundated wetlands, the seasonally inundated wetlands had relatively low observed and
292 simulated CH₄ emissions due to the significant influences of the water table level on CH₄ emissions (e.g., Hatano, 2019;
293 Zhang *et al.*, 2019). The CH₄ emissions simulated by the CNMM-DNDC were determined by the processes of production,
294 oxidation and transpiration under the concept of a CH₄ balloon. The unsaturated soil with moisture levels ranging from 0.41
295 to 0.98 WFPS resulted in a small CH₄ balloon and thus reduced CH₄ production. At the same time, relatively dry conditions
296 caused the upper soil layer to act as an efficient oxidative methanotrophic barrier for the diffusion of CH₄ from the subsoil
297 and thus decreased CH₄ emissions (Kandel *et al.*, 2018; Tan *et al.*, 2020). In addition, the highly fluctuating CH₄ emissions
298 simulated by the modified model were also attributed to the high dependency of CH₄ production on soil moisture, which
299 controlled the size of the CH₄ balloon. Theoretically, the CH₄ emissions simulated by the original model should not have
300 been higher than those simulated by the modified model due to the lower predicted soil moisture level. The overestimated
301 CH₄ emissions simulated by the original model were mainly attributed to the overestimated soil temperature due to their
302 influences on mineralized substrates for CH₄ production, as well as the processes of CH₄ production. This result implies that
303 global warming may trigger intensive CH₄ emissions from degraded wetlands, which could partly serve as a trade-off for the
304 decreased CH₄ emissions due to the lower water table level in degraded wetlands. Both observations and simulations showed
305 that the CH₄ uptake in alpine forests was higher than that in alpine meadows, which was mainly attributed to the high SOC
306 content and low soil clay fraction of the alpine forests in the simulation. Methane uptake by upland soils is a biological
307 process governed by the availability of CH₄ and oxygen as well as the activity and quantity of methanotrophic bacteria in
308 soils (e.g., Liu *et al.*, 2007; Zhang *et al.*, 2014). In the model, the simulated CH₄ uptake was positively related to the SOC
309 content, which is closely related to the population size of methanotrophic bacteria. On the other hand, soil permeability
310 affects gas diffusion into the soil and thus CH₄ uptake (e.g., Liu *et al.*, 2007). For the CNMM-DNDC, the clay fraction,



311 which is regarded as a key factor regulating soil permeability, showed a negative relationship with CH₄ uptake in the model.
312 Thus, the SOC content, as well as the soil clay fraction, contributed to the differences in CH₄ uptake from alpine meadows
313 and forests. As the simulated dynamic characteristics of CH₄ uptake were primarily regulated by soil temperature and
314 moisture, the effects of low soil temperature (< 0.0 °C) on CH₄ uptake rates resulted in obvious underestimations in the
315 dormant season for both alpine meadows and forests. Therefore, an improved parameterization for simulating CH₄ uptake
316 under low soil temperatures is required for the model to better capture the dynamics of CH₄ uptake in the dormant season.

317 **4.3 Model performance in simulating N₂O fluxes**

318 In comparison, the N₂O emissions from the alpine wetlands and forests were higher than those from the alpine
319 meadows for both the observations and simulations due to the high SOC content and nitrogen availability. Natural wetlands
320 are large carbon reserves and play a crucial role in mitigating global warming (e.g., Deng *et al.*, 2014; Kang *et al.*, 2020; Tan
321 *et al.*, 2020). The intentional drainage of annually inundated wetlands alters not only the water regime but also nutrient
322 availability (e.g., Hoffmann *et al.*, 2016). The simulated relatively low soil moisture for the alpine wetlands stimulated the
323 decomposition of SOC and nitrogen (or peat oxidation) under aerobic conditions, thus improving nitrogen mineralization for
324 nitrification and denitrification and enhancing N₂O emissions (e.g., Tan *et al.*, 2020; Zhang *et al.*, 2020). The intensive N₂O
325 emissions simulated by the original model resulted from the overestimated soil temperature for the alpine wetlands, as well
326 as the lower predicted soil moisture, which not only facilitated soil mineralization but also provided favorable oxygen
327 conditions for N₂O production. This result also indicates that global warming may significantly increase N₂O emissions from
328 seasonally inundated wetlands. Field studies showed that high SOC concentrations could stimulate the processes of
329 mineralization and nitrification in the forests (e.g., Li *et al.*, 2005; Yao *et al.*, 2019). The model input of soil organic matter
330 measured in the observed alpine forests was more than twice that in the observed alpine meadows. Thus, the high SOC
331 content at the alpine forest site provided more available nitrogen through mineralization and thus stimulated the nitrification
332 processes in the simulation. Furthermore, the seasonal grazing that occurred in the alpine meadows resulted in constant loss
333 of available nitrogen and thus hindered the N₂O emissions from the biological processes in the simulation. The soil freeze-
334 thaw cycles that occurred in seasonally frozen regions, which were included in the modified CNMM-DNDC, not only
335 increased the availability of nitrogen and carbon substrates by disrupting of soil aggregates but also affected the structure,
336 population and activity of the microbes, and thus influencing the emissions of N₂O (e.g., Song *et al.*, 2019). The model set
337 threshold values of soil temperature to trigger the decomposition of microbes during the freezing period and stimulate the
338 production of NO, N₂O and N₂ using substrates derived from microbial decomposition during the thawing period. However,
339 the dynamics of peak emissions due to freeze-thaw cycles were inconsistent with those from the field observations. Thus,
340 improvements are required to optimize the parameterization scheme to better capture the dynamic characteristics. In addition,
341 the peak emissions during the freeze-thaw period were not captured by the original model due to the significantly
342 overestimated soil temperature. The low evaluation statistics for the daily fluxes, especially for the alpine forests, were also
343 attributed to the underestimation of background emissions, which resulted from both measurement errors due to low fluxes



344 around detection limits and model deficiencies in the simulation of tight nitrogen cycling in natural ecosystems. The model
345 performances of simulating various variables for three typical alpine ecosystems in the Rierlangshan catchment imply that
346 the modified CNMM-DNDC can be applied to predict the thermal dynamics, hydrology, nitrogen and carbon cycling and
347 related greenhouse gas emissions in seasonally frozen regions.

348 **4.4 Implications for degraded alpine ecosystems**

349 The typical natural wetland alpine ecosystems, which are annually inundated, act as greenhouse gas sinks or are
350 neutral (e.g., Cai., 2012; Tan *et al.*, 2020). A previous study showed that more than 90% of the annually inundated wetlands
351 on the TP have been degraded and become seasonally inundated or wet alpine meadows due to intentional drainage for
352 grazing since the 1960s (Wei *et al.*, 2015). Both the observations and simulations showed that in comparison to annually
353 inundated wetlands, wetland degradation induced by drainage stimulated N₂O emissions to a small extent but reduced CH₄
354 emissions to a large extent. Thus, compared to that from natural wetlands, the aggregate emissions of CH₄ and N₂O from
355 degraded wetlands were largely reduced but still higher than those of adjacent wet alpine meadows. These results were
356 consistent with the field observations of CH₄ and N₂O emissions along different water table transects in the Zoige peatland,
357 which were primarily driven by soil water content and SOC (Zhang *et al.*, 2020). The decline in the water table induced by
358 intentional drainage resulted in recessive succession of the vegetation for the Zoige wetland with a typical mode of marsh,
359 marsh meadow and meadow (Xiang *et al.*, 2009). Thus, one may deduce that the degradation of annually inundated wetlands
360 at a large-scale might have greatly reduced the aggregate emissions of CH₄ and N₂O from the Zoige wetland, especially for
361 CH₄. However, a recent meta-analysis showed that the reduction in the aggregate emissions of CH₄ and N₂O due to draining
362 may be completely offset by the decreased net CO₂ uptake (Tan *et al.*, 2020). For natural wetlands, anaerobic conditions
363 under high a water table inhibit litter decomposition, and thus, a large amount of organic matter is sequestered (Nahlik and
364 Fennessy, 2016). When the annually inundated wetlands degrade to seasonally inundated wetlands or meadows, the rate of
365 peat soil oxidation is enhanced, thus significantly increasing ecosystem respiration and resulting in a shift from net sinks of
366 greenhouse gas emissions to notable sources (Tan *et al.*, 2020). Consistent with the results of the meta-analysis, the
367 simulation showed that the loss rate of SOC (consisting of microbes, humads and humus) was much higher for degraded
368 wetlands than for other typical alpine ecosystems. These results also indicate the large risk of soil carbon loss due to
369 intentional drainage, which has been sequestered for a long time. The simulation by the modified CNMM-DNDC showed
370 that the model has the capacity to simulate hydro-biogeochemical processes in seasonally frozen regions for various alpine
371 ecosystems.

372 **5 Conclusions**

373 To apply the process-oriented hydro-biogeochemical model Catchment Nutrient Management Model - DeNitrification-
374 DeComposition (CNMM-DNDC) in seasonally frozen regions, an improved module of soil thermal dynamics for describing



375 the soil thermal regime in the presence of freeze-thaw cycles was incorporated in this study. Using the unique experimental
376 dataset obtained for the Rierlangshan catchment with the typical alpine wetland, meadow and forest ecosystems, the
377 modified model was evaluated for simulating soil thermal dynamics (soil profile temperature), topsoil moisture and methane
378 (CH₄) and nitrous oxide (N₂O) fluxes for the three ecosystems and the effects of wetland degradation on CH₄ and N₂O fluxes
379 in seasonally frozen regions of the Tibetan Plateau. The simulations showed acceptable performances for the above variables,
380 indicating the capacity of the modified model to simulate the processes of thermal dynamics, hydrology, and nitrogen and
381 carbon cycling in seasonally frozen regions. Both the observed and simulated CH₄ and N₂O fluxes from alpine wetlands and
382 meadows, as well as the results from the simulated annually inundated wetlands, indicate that wetland degradation due to
383 intentional drainage resulted in a significant reduction in the aggregate emissions of CH₄ and N₂O. Reduced soil moisture
384 and lower soil organic carbon contents were the primary factors for the decreased aggregate emissions of CH₄ and N₂O. In
385 addition, the simulated intensive losses of soil organic carbon for the alpine wetlands suggest the inhibitory effects of
386 wetland degradation on soil carbon sequestration but stimulatory influences on net greenhouse gas emissions. This study
387 implies that hydro-biogeochemical model, such as the modified CNMM-DNDC, are able to predict soil thermal dynamics
388 and cycling of nitrogen and carbon in seasonally frozen regions with an improved physical-based soil thermal module.

389 **Data availability**

390 The model, input and output databases can be obtained from the first author and all the observed data sets used in this study
391 can be available from the co-authors.

392 **Author contribution**

393 Zheng, X. and Zhang, W. contributed to developing the idea and enhancing the science of this study. Zhang, W. improved
394 the scientific processes of the model, implemented the model simulations and prepared the manuscript with contributions
395 from all co-authors. Li, S. improved the model structure for standard input. Yao, Z., Zhang, H., Ma, L., Wang, K., Wang, R.
396 and Liu, C. designed and carried out the field experiments. Han, S. collected and established the input database for modelling.
397 Deng, J and Li, Y contributed to the modification of the model and the improvement of the manuscript.

398 **Competing interests**

399 The authors declare that they have no conflict of interest.



400 Acknowledgement

401 This study was jointly supported by the National Key R&D Program of China (2016YFA0602303), the Chinese Academy of
402 Sciences (ZDBS-LY-DQC007), the National Key Scientific and Technological Infrastructure project “Earth System Science
403 Numerical Simulator Facility” (EarthLab) and the National Natural Science Foundation of China (41603075, 41861134029).

404 References

- 405 Bechmann, M., 2014. Long-term monitoring of nitrogen in surface and subsurface runoff from small agricultural dominated
406 catchments in Norway. *Agric. Ecosyst. Environ.* 198, 13–24.
- 407 Bosch, N., Allan, J., Dolan, D., Han, H., Richards, R., 2011. Application of the Soil and Water Assessment Tool for six
408 watersheds of Lake Erie: Model parameterization and calibration. *J. Great Lakes Res.* 37, 263–271.
- 409 Breuer, L., VachÉ, K., Julich, S., Frede, H., 2010. Current concepts in nitrogen dynamics for mesoscale catchments. *Hydrol.*
410 *Sci. J.-J. Sci. Hydrol.* 53, 1059–1074.
- 411 Canfield, D., Glazer, A., Falkowski, P., 2010. The evolution and future of Earth's nitrogen cycle. *Science* 330, 192–196.
- 412 Cai, Z., 2012. Greenhouse gas budget for terrestrial ecosystems in China. *Sci. China-Earth Sci.* 55, 173–182.
- 413 Castellano, M., Lewis, D., Kaye, J., 2013. Response of soil nitrogen retention to the interactive effects of soil texture,
414 hydrology, and organic matter. *J. Geophys. Res.-Biogeosci.* 118, 280–290.
- 415 Chen, D., Li, Y., Grace, P., Mosier, A., 2008. N₂O emissions from agricultural lands: a synthesis of simulation approaches.
416 *Plant Soil* 309, 169–189.
- 417 Cheng, K., Ogle, S., Parton, W., Pan, G., 2014. Simulating greenhouse gas mitigation potentials for Chinese Croplands using
418 the DAYCENT ecosystem model. *Glob. Change Biol.* 20, 948–962.
- 419 Collins, A., Zhang, Y., Winter, M., Inman, A., Jones, J., Johnes, P., Cleasby, W., Vrain, E., Lovett, A., Noble, L., 2016.
420 Tackling agricultural diffuse pollution: What might uptake of farmer-preferred measures deliver for emissions to water
421 and air? *Sci. Total Environ.* 547, 269–281.
- 422 Congreves, K., Grant, B., Dutta, B., Smith, W., Chantigny, M., Rochette, Desjardins, R., 2016. Prediction ammonia
423 volatilization after field application of swine slurry: DNDC model development, *Agric. Ecosyst. Environ.* 219, 179–189.
- 424 Cui, Z., Zhang, H., Chen, X., Zhang, C., Ma, W., Huang, C., Zhang, W., Mi, G., Miao, Y., Li, X., Gao, Q., Yang, J., Wang,
425 Z., Ye, Y., Guo, S., Lu, J., Huang, J., Lv, S., Sun, Y., Liu, Y., Peng, X., Ren, J., Li, S., Deng, X., Shi, X., Zhang, Q.,
426 Yang, Z., Tang, L., Wei, C., Jia, L., Zhang, J., He, M., Tong, Y., Tang, Q., Zhong, X., Liu, Z., Cao, N., Kou, C., Ying,
427 H., Yin, Y., Jiao, X., Zhang, Q., Fan, M., Jiang, R., Zhang, F., Dou, Z., 2018. Pursuing sustainable productivity with
428 millions of smallholder farmers. *Nature* 555, 363–366.
- 429 Deng, J., Li, C., Frohling, S., Zhang, Y., Bäckstrand, K., Crill, P., 2014. Assessing effects of permafrost thaw on C fluxes
430 based on multiyear modeling across a permafrost thaw gradient at Stordalen, Sweden. *Biogeosciences* 11, 4753–4770.
- 431 Dong, Z., Hu, G., Yan, C., Wang, W., Lu, J., 2010. Aeolian desertification and its causes in the Zoige Plateau of China's
432 Qinghai–Tibetan Plateau. *Environ. Earth Sci.* 59, 1731–1740.
- 433 Dubache, G., Li, S., Zheng, X., Zhang, W., Deng, J., 2019. Modeling ammonia volatilization following urea application to
434 winter cereal fields in the United Kingdom by improving a biogeochemical model, *Sci. Total Environ.* 660, 1403–1418.
- 435 Fenner, N., Freeman, C., 2011. Drought-induced carbon loss in peatlands. *Nat. Geosci.* 4, 895–900.
- 436 Foereid, B., Barthram, G., Marriott, C., 2007. The CENTURY model failed to simulate soil organic matter development in
437 an acidic grassland. *Nutr. Cycl. Agroecosyst.* 78, 143–153.
- 438 Galloway, J., Dentener, F., Capone, D., Boyer, E., Howarth, R., Seitzinger, S., Asner, G., Cleveland, C., Green, P., Holland,
439 E., Karl, D., Michaels, A., Porter, J., Townsend, A., Vorosmarty, C., 2004. Nitrogen Cycles: past, present, and future.
440 *Biogeochemistry* 70, 153–226.
- 441 Galloway, J., Townsend, A., Erismann, J., Bekunda, M., Cai, Z., Freney, J., Martinelli, L., Seitzinger, S., Sutton, M., 2008.
442 Transformation of the nitrogen cycle: recent trends, questions, and potential solutions. *Science* 320, 889–892.
- 443 Guo, L., Zhang, Y., Bohn, T., Zhao, L., Li, J., Liu, Q., Zhou, B., 2015. Frozen soil degradation and its effects on surface
444 hydrology in the northern Tibetan Plateau. *J. Geophys. Res. Atmos.* 120, 8276–8298.



- 445 Haas, E., Klatt, S., Fröhlich, A., Kraft, P., Werner, C., Kiese, R., Grote, R., Breuer, L., Butterbach-Bahl, K., 2012.
446 LandscapeDNDC: a process model for simulation of biosphere–atmosphere–hydrosphere exchange processes at site and
447 regional scale. *Landsc. Ecol.* 28, 615–636.
- 448 Hatano, R., 2019. Impact of land use change on greenhouse gases emissions in peatland: a review. *Int. Agrophys.* 33, 167–
449 173.
- 450 Holzworth, D., Huth, N., deVoil, P., Zurcher, E., Herrmann, N., McLean, G., Chenu, K., van Oosterom, E., Snow, V.,
451 Murphy, C., Moore, A., Brown, H., Whish, J., Verrall, S., Fainges, J., Bell, L., Peake, A., Poulton, P., Hochman, Z.,
452 Thorburn, P., Gaydon, D., Dalgliesh, N., Rodriguez, D., Cox, H., Chapman, S., Doherty, A., Teixeira, E., Sharp, J.,
453 Cichota, R., Vogeler, I., Li, F., Wang, E., Hammer, G., Robertson, M., Dimes, J., Whitbread, A., Hunt, J., van Rees, H.,
454 McClelland, T., Carberry, P., Hargreaves, J., MacLeod, N., McDonald, C., Harsdorf, J., Wedgwood, S., Keating, B.,
455 2014. APSIM – Evolution towards a new generation of agricultural systems simulation. *Environ. Modell. Softw.* 62,
456 327–350.
- 457 Hugelius, G., Loisel, J., Chadburn, S., Jackson, R., Jones, M., MacDonald, G., Marushchak, M., Olefeldt, D., Maara, P.,
458 Siewert, M., Treat, C., Turetsky, M., Voigt, C., Yu, Z., 2020. Large stocks of peatland carbon and nitrogen are
459 vulnerable to permafrost thaw. *Proc. Natl. Acad. Sci. U. S. A.* doi: 10.1073/pnas.1916387117
- 460 Intergovernmental Panel on Climate Change (IPCC): Climate Change 2013: The Physical Science Basis, Contribution of
461 Working Group I to the Fifth Assessment Report of the Intergovernmental Panel on Climate Change (eds. Stocker TF,
462 Qin D, Plattner G-K, et al.), Cambridge University Press, Cambridge, United Kingdom and New York, NY, USA, 2013.
- 463 Jiang, H., Yi, Y., Zhang, W., Yang, K., Chen, D., 2020. Sensitivity of soil freeze/thaw dynamics to environmental conditions
464 at different spatial scales in the central Tibetan Plateau. *Sci. Total Environ.* 734, 139261. doi:
465 org/10.1016/j.scitotenv.2020.139261
- 466 Jiang, Z., 2010. Analysis on the establishment conditions of the square sum decomposition formular of regression model, *J.*
467 *Industr. Techn. Econ.*, 29(4), 116–119 (in Chinese).
- 468 Ju, X., Xing, G., Chen, X., Zhang, S., Zhang, L., Liu, X., Cui, Z., Yin, B., Christie, P., Zhu, Z., Zhang, F., 2009. Reducing
469 environmental risk by improving N management in intensive Chinese agricultural systems. *Proc. Natl. Acad. Sci. U.*
470 *S. A.* 106, 3041–3046.
- 471 Kandel, T., Lærke, P., Elsgaard, L., 2018. Annual emissions of CO₂, CH₄ and N₂O from a temperate peat bog: comparison of
472 an undrained and four drained sites under permanent grass and arable crop rotations with cereals and potato. *Agric. For.*
473 *Meteorol.* 256–257, 470–481.
- 474 Kang, X., Li, Y., Wang, J., Yan, L., Zhang, X., Wu, H., Yan, Z., Zhang, K., Hao, Y., 2020. Precipitation and temperature
475 regulate the carbon allocation process in alpine wetlands: quantitative simulation. *J. Soils Sediments* 20, 3300–3315.
- 476 Keiluweit, M., Wanzek, T., Kleber, M., Nico, P., Fendorf, S., 2017. Anaerobic microsites have an unaccounted role in soil
477 carbon stabilization. *Nat. Commun.* 8. doi: 10.1038/s41467-017-01406-6
- 478 Kolb, S., Horn, M., 2012. Microbial CH₄ and N₂O consumption in acidic wetlands. *Front. Microbiol.* 3, 78. doi:
479 10.3389/fmicb.2012.00078
- 480 Li, B., Yu, Z., Liang, Z., Song, K., Li, H., Wang, Y., Zhang, W., Acharya, K., 2014. Effects of climate variations and human
481 activities on runoff in the Zoige alpine wetland in the eastern edge of the Tibetan Plateau. *J. Hydrol. Eng.* 19, 1026–
482 1035.
- 483 Li, C., 2007. Quantifying greenhouse gas emissions from soils: scientific basis and modeling approach. *Soil Sci. Plant Nutr.*
484 53, 344–352.
- 485 Li, C., Frolking, S., Butterbach-Bahl, K., 2005. Carbon sequestration in arable soils is likely to increase nitrous oxide
486 emissions, offsetting reductions in climate radiative forcing. *Clim. Change* 72, 321–338.
- 487 Li, S., Zheng, X., Zhang, W., Han, S., Deng, J., Wang, K., Wang, R., Yao, Z., Liu, C., 2019. Modeling ammonia
488 volatilization following the application of synthetic fertilizers to cultivated uplands with calcareous soils using an
489 improved DNDC biogeochemistry model. *Sci. Total Environ.* 660, 931–946.
- 490 Li, Y., White, R., Chen, D., Zhang, J., Li, B., Zhang, Y., Huang, Y., Edis, R., 2007. A spatially referenced water and
491 nitrogen management model (WNMM) for (irrigated) intensive cropping systems in the North China Plain. *Ecol. Model.*
492 203, 395–423.



- 493 Liu, C., Holst, J., Brüggemann, N., Butterbach-Bahl, K., Yao, Z., Yue, J., Han, S., Han, X., Krümmelbein, J., Horn, R.,
494 Zheng, X., 2007. Winter-grazing reduces methane uptake by soils of a typical semi-arid steppe in Inner Mongolia,
495 China. *Atmos. Environ.* 41, 5948–5958.
- 496 Liu, S., Xie, Z., Zeng, Y., Liu, B., Li, R., Wang, Y., Wang, L., Qin, P., Jia, B., Xie, J., 2019. Effects of anthropogenic
497 nitrogen discharge on dissolved inorganic nitrogen transport in global rivers. *Glob. Change Biol.* 25, 1493–1513.
- 498 Ma, L., Yao, Z., Zheng, X., Zhang, H., Wang, K., Zhu, B., Wang, R., Zhang, W., Liu, C., 2018. Increasing grassland
499 degradation stimulates the non-growing season CO₂ emissions from an alpine meadow on the Qinghai-Tibetan Plateau.
500 *Environ. Sci. Pollut. Res.* 25, 26576–26591.
- 501 McClain, M., Boyer, E., Dent, C., Gergel, S., Grimm, N., Groffman, P., Hart, S., Harvey, J., Johnston, C., Mayorga, E., 2003.
502 Biogeochemical hot spots and hot moments at the interface of terrestrial and aquatic ecosystems. *Ecosystems* 6, 301–
503 312.
- 504 Moriasi, D., Arnold, J., Van Liew, M., Bingner, R., Harmel, R., Veith, T., 2007. Model evaluation guidelines for systematic
505 quantification of accuracy in watershed simulation, *T. Am. Soc. Agr. Biol. Eng.* 50, 885–900.
- 506 Nahlik, A., Fennessy, M., 2016. Carbon storage in US wetlands. *Nat. Commun.* 7, 13835. doi: 10.1038/ncomms13835
- 507 Nash, J., Sutcliffe, J., 1970. River flow forecasting through conceptual models: part I- a discussion of principles, *J. Hydrol.*
508 10, 282–290.
- 509 Piao, S., Fang, J., Ciais, P., Peylin, P., Huang, Y., Sitch, S., Wang, T., 2009. The carbon balance of terrestrial ecosystems in
510 China. *Nature* 458, 1009–1013.
- 511 Pohlert, T., Huisman, J., Breuer, L., Frede, H., 2007. Integration of a detailed biogeochemical model into SWAT for
512 improved nitrogen predictions—Model development, sensitivity, and GLUE analysis. *Ecol. Model.* 203, 215–228.
- 513 Pollack, H., Chapman, D., 1977. On the regional variation of heat flow, geotherms, and lithospheric thickness.
514 *Tectonophysics* 38, 279–296.
- 515 Schroeck, A., Gaube, V., Haas, E., Winiwarter, W., 2019. Estimating nitrogen flows of agricultural soils at a landscape level
516 - A modelling study of the Upper Enns Valley, a long-term socio-ecological research region in Austria. *Sci. Total*
517 *Environ.* 665, 275–289.
- 518 Schuur, E., McGuire, A., Schadel, C., Grosse, G., Harden, J., Hayes, D., Hugelius, G., Koven, C., Kuhry, P., Lawrence, D.,
519 Natali, S., Olefeldt, D., Romanovsky, V., Schaefer, K., Turetsky, M., Treat, C., Vonk, J., 2015. Climate change and the
520 permafrost carbon feedback. *Nature* 520, 171–179.
- 521 Seitzinger, S., 2008. Nitrogen cycle - Out of reach. *Nature* 452, 162–163.
- 522 Song, L., Yao, Y., Lin, L., Gao, W., Cai, T., Liang, H., Gao, D., 2019. The potential source of nitrous oxide in the pristine
523 riparian marsh during freeze-thaw cycles, case study in Northeast China. *Ecol. Eng.* 134, 18–25.
- 524 Tan, L., Ge, Z., Zhou, X., Li, S., Li, X., Tang, J., 2020. Conversion of coastal wetlands, riparian wetlands, and peatlands
525 increases greenhouse gas emissions: a global meta-analysis, *Glob. Change Biol.* 26, 1638–1653.
- 526 Vereecken, H., Schnepf, A., Hopmans, J., Javaux, M., Or, D., Roose, T., Vanderborght, J., Young, M., Amelung, W.,
527 Aitkenhead, M., Allison, S., Assouline, S., Baveye, P., Berli, M., Brüggemann, N., Finke, P., Flury, M., Gaiser, T.,
528 Govers, G., Ghezzehei, T., Hallett, P., Hendricks Franssen, H., Heppell, J., Horn, R., Huisman, J., Jacques, D., Jonard,
529 F., Kollet, S., Lafolie, F., Lamorski, K., Leitner, D., McBratney, A., Minasny, B., Montzka, C., Nowak, W., Pachepsky,
530 Y., Padarian, J., Romano, N., Roth, K., Rothfuss, Y., Rowe, E., Schwen, A., Šimůnek, J., Tiktak, A., Van Dam, J., van
531 der Zee, S., Vogel, H., Vrugt, J., Wöhling, T., Young, I., 2016. Modeling Soil Processes: Review, Key Challenges, and
532 New Perspectives. *Vadose Zone J.* 15, doi:10.2136/vzj2015.2009.0131.
- 533 Wei, D., Xu-Ri, T., Tarchen, T., Dai, D., Wang, Y., Wang, Y., 2015. Revisiting the role of CH₄ emissions from alpine wetlands
534 on the Tibetan Plateau: evidence from two in situ measurements at 4758 and 4320 m above sea level. *J. Geophys. Res.-*
535 *Biogeosci.* 120, 1741–1750.
- 536 Wu, Y., Liu, S., Qiu, L., Sun, Y., 2016. SWAT-DayCent coupler: An integration tool for simultaneous hydro-
537 biogeochemical modeling using SWAT and DayCent. *Environ. Modell. Softw.* 86, 81–90.
- 538 Willmott, C., Matsuura, K., 2005. Advantages of the mean absolute error (MAE) over the root mean square error (RMSE)
539 in assessing average model performance, *Clim. Res.*, 30, 79–82.
- 540 Xiang, S., Guo, R., Wu, N., Sun, S., 2009. Current status and future prospects of Zoige Marsh in Eastern Qinghai-Tibet
541 Plateau. *Ecol. Eng.* 35, 553–562.



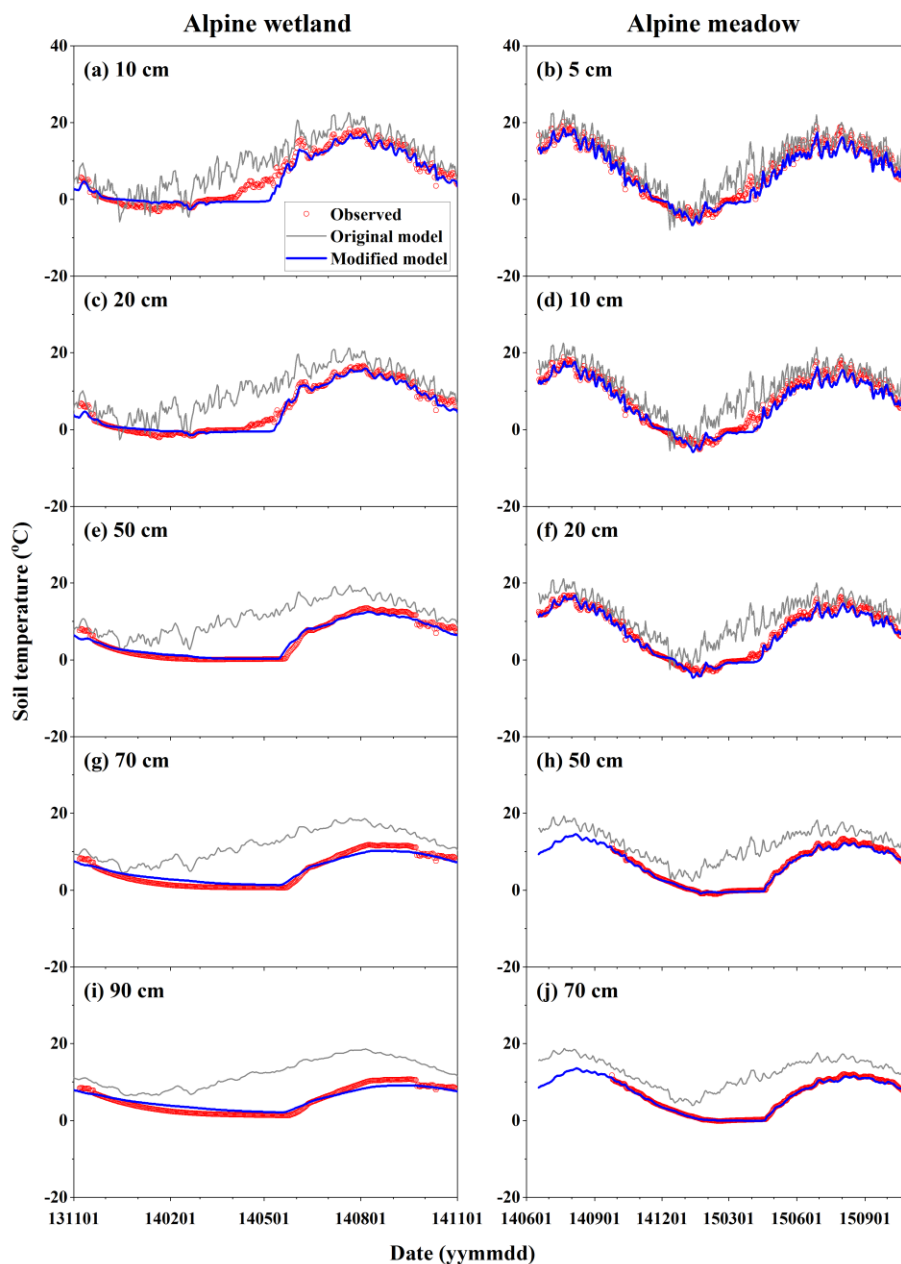
- 542 Yao, Z., Ma, L., Zhang, H., Zheng, X., Wang, K., Zhu, B., Wang, R., Wang, Y., Zhang, W., Liu, C., Butterbach-Bahl, K.,
543 2019. Characteristics of annual greenhouse gas flux and NO release from alpine meadow and forest on the eastern
544 Tibetan Plateau. *Agric. For. Meteorol.* 272-273, 166-175.
- 545 Zhang, H., Yao, Z., Ma, L., Zheng, X., Wang, R., Wang, K., Liu, C., Zhang, W., Zhu, B., Tang, X., Hu, Z., Han, S., 2019.
546 Annual methane emissions from degraded alpine wetlands in the eastern Tibetan Plateau. *Sci. Total Environ.* 657,
547 1323–1333.
- 548 Zhang, H., Yao, Z., Wang, K., Zheng, X., Ma, L., Wang, R., Liu, C., Zhang, W., Zhu, B., Tang, X., Hu, Z., Han, S., 2018a.
549 Annual N₂O emissions from conventionally grazed typically alpine grass meadows in the eastern Qinghai-Tibetan
550 Plateau. *Sci. Total Environ.* 625, 885–899.
- 551 Zhang, W., Li, Y., Zhu, B., Zheng, X., Liu, C., Tang, J., Su, F., Zhang, C., Ju, X., Deng, J., 2018b. A process-oriented hydro-
552 biogeochemical model enabling simulation of gaseous carbon and nitrogen emissions and hydrologic nitrogen losses
553 from a subtropical catchment. *Sci. Total Environ.* 616–617, 305–317.
- 554 Zhang, W., Liu, C., Zheng, X., Fu, Y., Hu, X., Cao, G., Butterbach-Bahl, K., 2014. The increasing distribution area of zokor
555 mounds weaken greenhouse gas uptakes by alpine meadows in the Qinghai–Tibetan Plateau. *Soil Biol. Biochem.* 71,
556 105–112.
- 557 Zhang, W., Liu, C., Zheng, X., Wang, K., Cui, F., Wang, R., Li, S., Yao, Z., Zhu, J., 2019. Using a modified DNDC
558 biogeochemical model to optimize field management of a multi-crop (cotton, wheat, and maize) system: a site-scale
559 case study in northern China. *Biogeosciences* 16, 2905–2922.
- 560 Zhang, W., Liu, C., Zheng, X., Zhou, Z., Cui, F., Zhu, B., Haas, E., Klatt, S., Butterbach-Bahl, K., Kiese, R., 2015.
561 Comparison of the DNDC, LandscapeDNDC and IAP-N-GAS models for simulating nitrous oxide and nitric oxide
562 emissions from the winter wheat-summer maize rotation system. *Agric. Syst.* 140, 1–10.
- 563 Zhang, W., Wang, J., Hu, Z., Li, Y., Yan, Z., Zhang, X., Wu, G., Yan, L., Zhang, K., Kang, X., 2020. The primary drivers of
564 greenhouse gas emissions along the water table gradient in the Zoige alpine peatland. *Water Air Soil Pollut.* 231: 224.
565 doi: org/10.1007/s11270-020-04605-y
- 566 Zhang, Y., Chen, W., Cihlar, J., 2003. A process-based model for quantifying the impact of climate change on permafrost
567 thermal regimes. *J. Geophys. Res.-Atmos.* 108, 4695.
- 568 Zhang, Y., Li, C., Trettin, C., Li, H., Sun, G., 2002. An integrated model of soil, hydrology, and vegetation for carbon
569 dynamics in wetland ecosystems. *Glob. Biogeochem. Cycle* 16, 1061.
- 570 Zhang, Y., Shao, Q., Ye, A., Xing, H., Xia, J., 2016. Integrated water system simulation by considering hydrological and
571 biogeochemical processes: model development, with parameter sensitivity and autocalibration. *Hydrol. Earth Syst. Sci.*
572 20, 529–553.
- 573 Zhu, Q., Castellano, M., Yang, G., 2018. Coupling soil water processes and the nitrogen cycle across spatial scales:
574 potentials, bottlenecks and solutions. *Earth-Sci. Rev.* 187, 248–258.
- 575 Zhu, Q., Schmidt, J.P., Bryant, R., 2012. Hot moments and hot spots of nutrient losses from a mixed land use watershed. *J.*
576 *Hydrol. Eng.* 414, 393–404.



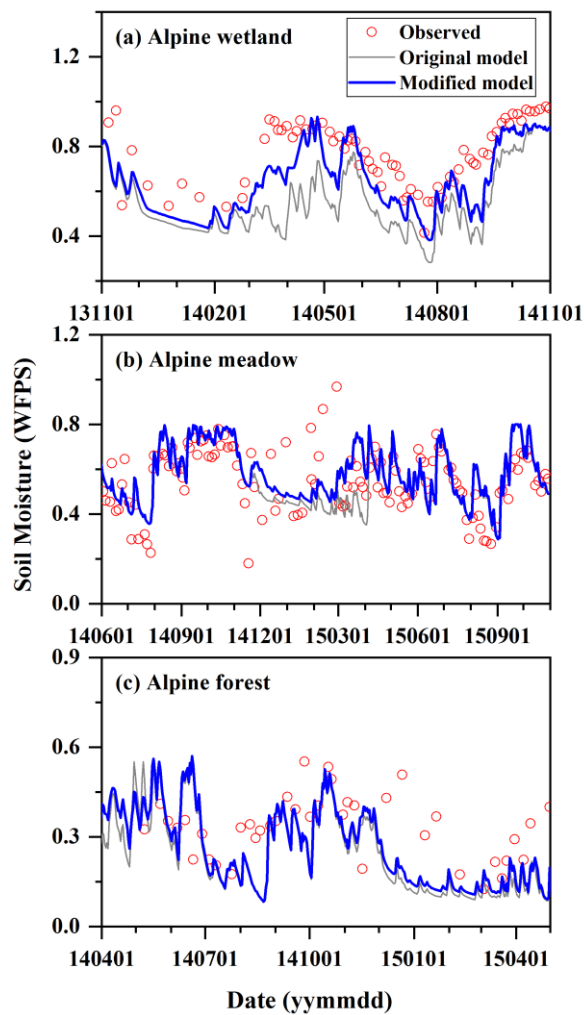
577 Table 1 Statistics of the validated variables by the modified CNMM-DNDC for three typical alpine ecosystems.
 578

Item	Ecosystem	<i>n</i>	IA		NSI		Slope		R^{2c}		P	
			O ^a	M ^b	O	M	O	M	O	M	O	M
Soil temperature												
5 cm	Meadow	500	0.90	0.96	0.82	0.95	0.84	1.09	0.89	0.96	< 0.001	< 0.001
	Forest	48	0.85	0.91	0.37	0.68	0.64	0.83	0.68	0.73	< 0.001	< 0.001
10 cm	Wetland	366	0.90	0.98	0.57	0.92	0.72	1.07	0.81	0.93	< 0.001	< 0.001
	Meadow	500	0.93	0.99	0.71	0.95	0.80	1.08	0.85	0.96	< 0.001	< 0.001
20 cm	Wetland	366	0.82	0.99	0.18	0.96	0.64	1.05	0.66	0.97	< 0.001	< 0.001
	Meadow	500	0.87	0.99	0.48	0.97	0.74	1.06	0.76	0.98	< 0.001	< 0.001
50 cm	Wetland	366	0.66	0.99	-1.01	0.97	0.51	1.05	0.43	0.97	< 0.001	< 0.001
	Meadow	401	0.70	1.00	-0.48	0.99	0.58	1.06	0.53	1.00	< 0.001	< 0.001
70 cm	Wetland	366	0.58	0.98	-2.23	0.93	0.47	1.05	0.38	0.93	< 0.001	< 0.001
	Meadow	401	0.64	1.00	-1.19	0.99	0.54	1.03	0.49	1.00	< 0.001	< 0.001
90 cm	Wetland	366	0.52	0.98	-4.07	0.90	0.44	1.03	0.36	0.90	< 0.001	< 0.001
Soil moisture												
Soil moisture	Wetland	74	0.63	0.83	-1.65	0.20	1.31	1.13	–	0.60	–	< 0.001
	Meadow	128	0.78	0.78	0.28	0.32	0.96	0.93	0.30	0.41	< 0.001	< 0.001
	Forest	40	0.48	0.49	-1.04	-0.80	1.21	1.19	–	–	–	–
Daily CH ₄ flux												
Daily CH ₄ flux	Wetland	180	0.37	0.74	-11.1	-0.73	0.46	0.87	–	–	–	–
	Meadow	168	0.87	0.88	0.42	0.38	1.09	0.94	0.44	0.39	< 0.001	< 0.001
	Forest	49	0.59	0.57	-2.79	-3.39	0.92	0.79	–	–	–	–
Daily N ₂ O flux												
Daily N ₂ O flux	Wetland	180	0.01	0.26	-323	-0.07	0.01	0.59	–	–	–	–
	Meadow	168	0.23	0.44	-0.16	-1.76	0.99	0.35	–	–	–	–
	Forest	58	0.47	0.47	-1.85	-1.64	0.44	0.47	–	–	–	–

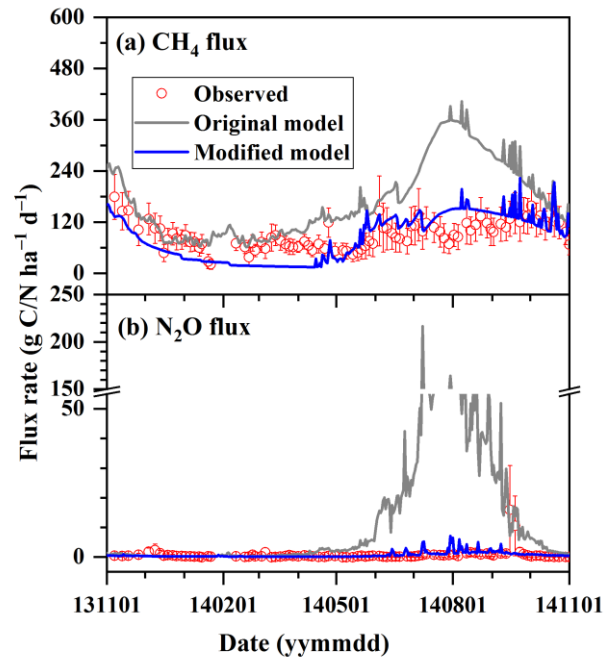
579 ^a O indicates the simulations by the original model. ^b M indicates the simulations by the modified model. ^c “–” indicated no
 580 value.



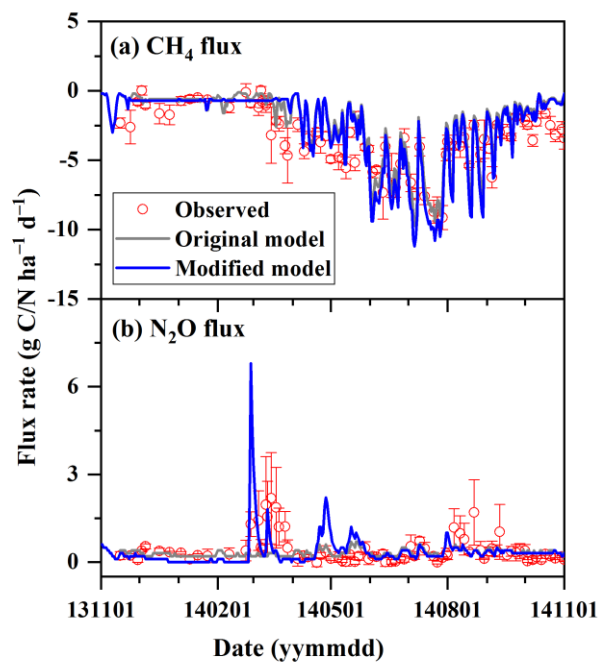
581
582 **Figure: 1** Observed and simulated daily profile soil temperature from the alpine wetlands and meadows by the original and
583 **modified models. The legends in panel a apply for all panels.**



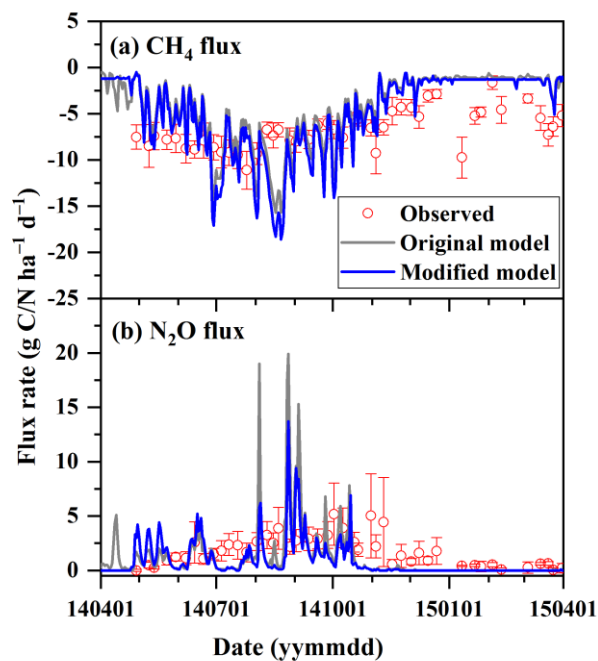
584
585 **Figure: 2** Observed and simulated daily topsoil (0–6 cm) moisture in the water-filled pore space (WFPS) from the alpine wetlands,
586 meadows and forests by the original and modified models. The legends in panel a apply for all panels.



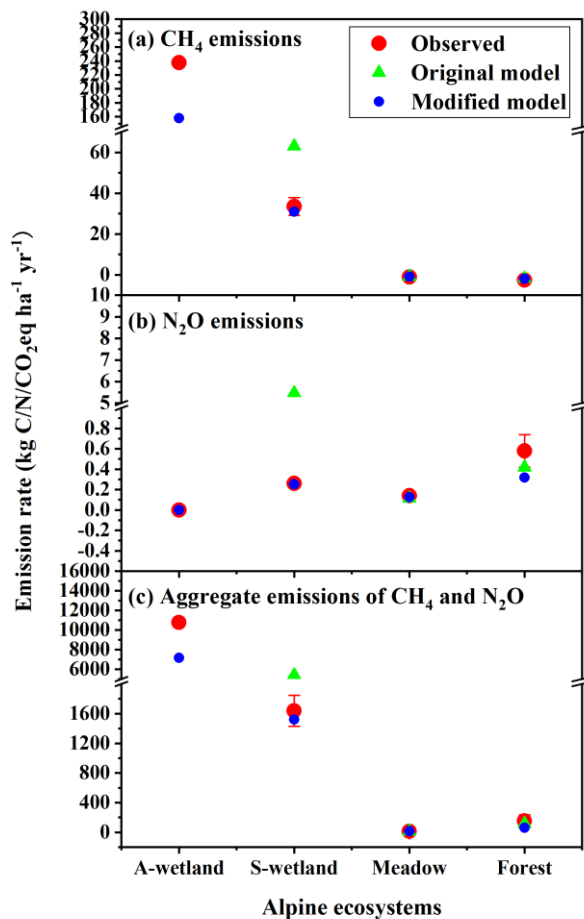
587
588 **Figure: 3** Observed and simulated daily methane (CH₄) and nitrous oxide (N₂O) fluxes from the alpine wetlands by the original
589 and modified models. The vertical bar for each observation indicates the standard error of six spatial replicates. The legends in
590 panel a apply for all panels.



591
592 **Figure: 4** Observed and simulated daily methane (CH₄) and nitrous oxide (N₂O) fluxes from the alpine meadows by the original
593 and modified models. The vertical bar for each observation indicates the standard error of four spatial replicates. The legends in
594 panel a apply for all panels.



595
596 **Figure: 5** Observed and simulated daily methane (CH₄) and nitrous oxide (N₂O) fluxes from the alpine forests by the original and
597 **modified models.** The vertical bar for each observation indicates the standard error of four spatial replicates. The legends in panel
598 **a** apply for all panels.



599

600 **Figure 6** Observed and simulated annual emissions of methane (CH₄), nitrous oxide (N₂O) and aggregate emissions of both from
601 the annually inundated wetlands (A-wetland), seasonally inundated wetlands (S-wetland), alpine meadows and forests. The
602 legends in panel a apply for all panels.